Automated Stem Angle Determination for Temporal Plant Phenotyping Analysis

Sruti Das Choudhury
University of Nebraska-Lincoln
School of Natural Resources and
Department of Computer Science and Engineering
S.D.Choudhury@unl.edu

Saptarsi Goswami
University of Calcutta
A.K.Choudhury School of Information Technology
saptarsi007@gmail.com

Srinidhi Bashyam
University of Nebraska-Lincoln
Department of Computer Science and Engineering
srinidhi.bashyam@gmail.com

Ashok Samal
University of Nebraska-Lincoln
Department of Computer Science and Engineering
samal@cse.unl.edu

Tala Awada
University of Nebraska-Lincoln
School of Natural Resources
tawada2@unl.edu

Abstract

Image-based plant phenotyping analysis refers to the monitoring and quantification of phenotyping traits by analyzing images of the plants captured by different types of cameras at regular intervals in a controlled environment. Extracting meaningful phenotypes for temporal phenotyping analysis by considering individual parts of a plant, e.g., leaves and stem, using computer-vision based techniques remains a critical bottleneck due to constantly increasing complexity in plant architecture with variations in self-occlusions and phyllotaxy. The paper introduces an algorithm to compute the stem angle, a potential measure for plants' susceptibility to lodging, i.e., the bending of stem of the plant. Annual yield losses due to stem lodging in the U.S. range between 5 and 25%. In addition to outright yield losses, grain quality may also decline as a result of stem lodging. The algorithm to compute stem angle involves the identification of leaf-tips and leaf-junctions based on a graph theoretic approach. The efficacy of the proposed method is demonstrated based on experimental analysis on a publicly available dataset called Panicoid Phenomap-1. A time-series clustering analysis is also performed on the values of stem angles for a significant time interval during vegetative stage life cycle of the maize plants. This analysis effectively summarizes the temporal patterns of the stem angles into three main groups, which provides further insight into genotype specific behavior of the plants. A comparison of genotypic purity using time series analysis establishes that the temporal variation of the stem angles is likely to be regulated by genetic variation under similar environmental conditions.

1. Introduction

High throughput plant phenotyping by analyzing image sequences captured by different imaging modalities, e.g., visible light, infra-red, near infra-red, fluorescent and hyperspectral, at regular intervals in a controlled environment has drawn attention of the researchers in recent times to aim for high yield of better quality crops with minimum resource utilization. Extraction of phenotypes with botanical importance by analyzing plant images has the desirable advantages of non-destructive phenotypic measurements of a large number of plants with little or no manual intervention in a relatively short period of time. It also enables the com-

putation of advanced phenotypes which are not possible to compute manually.

Image-based plant phenotyping analysis has been categorized either as holistic or component [3]. Holistic analysis considers the whole plant as a single object to measure its geometrical shape attributes, e.g., height of the bounding rectangle characterizes plant height, width of the minimum enclosing bounding circle at the top view characterizes plant width and area of the convex-hull provides information on size of the plant. Two advanced holistic phenotypes are introduced in [3], namely, bi-angular convex-hull area ratio and plant aspect ratio, which respectively provide information on phyllotaxy, i.e., arrangements of leaves around the stem, and canopy architecture.

Component analysis considers the individual parts of a plant, e.g., stem, leaf, fruit and flower. Plants are the constantly changing organisms with increasing complexity in the architecture and exhibit variations in self-occlusions and phyllotaxy. Hence, extraction of component phenotypes and their temporal behavior analysis over a significant time duration of the life cycle, essentially requires advanced computer vision techniques for plant body-part detection and labeling in the presence of various challenging factors, e.g., self-occlusions and illumination variations.

Recent image-based plant phenotyping methods have mainly considered Arabidopsis (*Arabidopsis thaliana*) and tobacco (*Nicotiana tabacum*) as the model plants for the study of leaf segmentation using 3-dimensional histogram cubes and superpixels [10], plant growth and chlorophyll fluorescence analysis exposed to abiotic stress conditions [5], automated plant segmentation using active contour model [7] and the rate of leaf growth monitoring following leaf tracking using infrared stereo image sequences [1]. In contrast, the motivation of this work is to develop new component phenotyes of the maize plants, which is one of the three main grain crops, along with rice and wheat, responsible for half of total world calorie consumption.

This paper introduces an algorithm to compute a component phenotype called stem angle for the determination and quantification of a plant's susceptibility to stem lodging. Stem lodging refers to the displacement of the stem away from the vertical axis, and is primarily caused by the excessive nitrogen and moisture content in the soil, shading, overpopulated field and fungal disease [8]. Lodging leads to low yield, and for the case of a maize plant, the yield is worst affected if the lodging occurs at the ear emergence stage. This paper also presents a novel direction to image-based plant phenotyping by investigating the temporal pattern of component phenotypes regulated by genotype using time series cluster analysis. The analysis is demonstrated using stem angle in this paper, however, it can be extended for any component phenotype.

The paper has the following novel research contributions: (a) it introduces a method for stem angle computation for temporal plant phenotyping using a graph theoretic approach; (b) it presents time-series cluster analysis to demonstrate the genetic influence on the temporal pattern of the stem angles over a significant time interval during vegetative stage life cycle; (c) it introduces a new direction of cluster purity analysis of component phenotypes; and (d) it provides comparisons of cluster behaviors based on angular histograms of the representative plants.

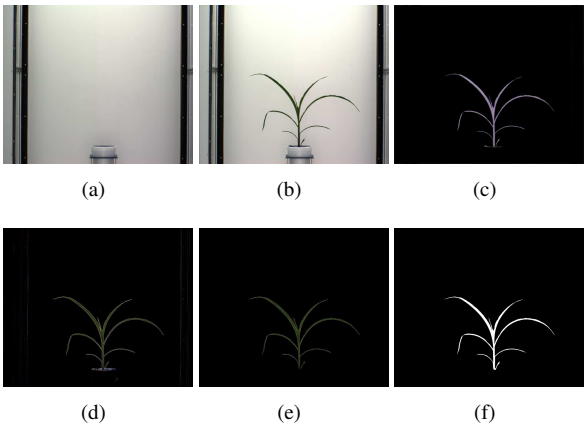

Figure 1. Illustration of two-phase segmentation process: (a) background image; (b) original image; (c) background subtraction using frame differencing technique; (d) green pixel superimposition; (e) background subtraction using color-based thresholding; and (f) binary image.

2. Stem angle computation

Stem angle computation (SAC) involves optimal view selection and stem angle measurement. The algorithm for SAC is provided in Algorithm 1.

2.1. Segmentation

A two-phase segmentation technique is used to extract the foreground, i.e., the plant, from the background which is defined as the part of the scene that remains static over the period of interest. Since the visible light imaging cabinet of the Lemnatec Scanalyzer 3D high throughput system has a fixed homogeneous background, the frame differencing technique of background subtraction is used to extract the plant from the background. However, successful execution of this technique requires the background and foreground images to be aligned with respect to scale and rotation. Hence, prior to applying frame differencing technique of background subtraction, we used automated image registration technique based on feature matching to account for change in zoom levels (resulting in scale variation) during the image capturing process. Figure 1(a) and (b) respectively show the background image and the original plant image. Figure 1(c) shows the plant extracted as a result of

Algorithm 1 SAC

Input: The plant sequence, i.e., P=$\{\alpha_1, \alpha_2,...,\alpha_n\}$, where n denotes the total number of imaging days. Since images are captured once daily for multiple side views, α_i =$\{v_{i,1}, v_{i,2},..., v_{i,p}\}$ $\forall$ i = 1, 2, ..., n, where p denotes the total number of available views of the plant for each day. Thus, n denotes the total number of images in P for a particular side view, and the total number of images in P is $n \times v$. For the sake of simplicity, we consider v=2 to correspond to two views, i.e., side view 0° and side view 90°.

Output: The numerical values of stem angle of the temporal image sequence of a plant for a particular view at which the line of sight of the camera is perpendicular to the line of axis of the leaves for the majority of the images in that image sequence.

Phase 1: view selection

$$\alpha_i = \begin{cases} 0° \text{if} \quad count(CV_{area}0) > count(CV_{area}90) \\ 90° \text{if} \quad count(CV_{area}90) > count(CV_{area}0) \end{cases}$$

where, $CV_{area}0$ and $CV_{area}90$ denote the area of the convex-hull of the image at side view 0° and side view 90°, respectively. If the area of the convex-hull for the majority of the images at side view 0° is higher than that of the images at side view 90°, all the images of side view 0° of P are chosen for subsequent analysis.

Phase 2: stem angle measurement

Iterate through the temporal image sequence of a plant consisting of n images.
for $j = 1 : n$ **do**
  Get the segmented image S_j using background subtraction and color-based thresholding techniques followed by connected component analysis.
  Compute the skeleton W_j of the segment S_j.
  Get the graphical representation G_j, of the skeleton W_j, with nodes and edges.
  Remove the spurious edges using a threshold of k pixels.
  Label the bottom most node in the graph G_j as 'base'.
  $N \leftarrow$ Add all the nodes, iteratively, by traversing the graph from the base along a connected path of nodes whose degree ≥ 3
  Label nodes in N as 'junctions'.
  Compute stem axis by linear regression curve fitting of all junctions.
  Compute the angle between the stem axis and the vertical axis as the stem angle.
end for

applying frame differencing technique of background subtraction. The resulting foreground image thus obtained, is often associated with undesirable soil pixels and the part of the background due to illumination variations as shown in Figure 1(d).

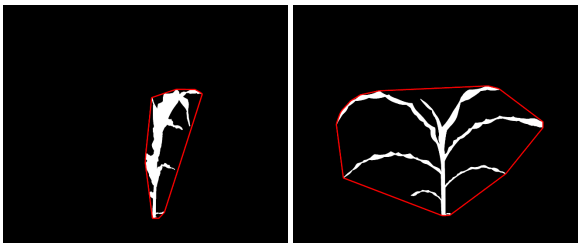

(a) (b)

Figure 2. Illustration of view selection: (a) plant image enclosed by convex-hull viewed at side view 0°; and (b) the same plant enclosed by convex-hull viewed at side view 90°.

To get rid of these noises, the pixels of the extracted foreground that correspond to green color of the original image, are assigned green color. After that, a color based segmentation technique is applied in the HSV color space to retain only green pixels, i.e., the pixels that correspond to the plant, using hue (range: 0.051-0.503), saturation (range: 0.102-0.804) and value (range: 0.000-0.786). The foreground thus obtained is shown in Figure 1(e). The extracted foreground is binarized using 2D Otsu automatic thresholding technique [6], which utilizes both the grey level information of each pixel and its spatial correlation information within the 2D neighborhood. The binary image is subjected to connected-component analysis involving morphological operation of erosion to remove noisy pixels and followed by dilation to fill up any small holes inside the plant image to give a single connected region as shown in Figure 1(f).

2.2. View selection

The successful execution of the proposed method requires all junctions (i.e., the point of contact of the leaves to the stem) are clearly visible. This is usually the case if the line of sight of the camera is perpendicular to the axis of the plant as evident in Figure 2. Figure 2(a) and (b) show the images of a maize plant from Panicoid Phenomap-1 at the side views 0° (where the junctions are not visible due to extreme leaf crossovers) and 90° (where all the junctions are clearly visible), respectively.

In order to select the desired view of the plant from the available p number of views, i.e., the view at which the line of sight of the camera is perpendicular to the axis of the plant, we compute area of the convex-hull of the plant for all days for p number of views. The view of the plant for which the area of the convex-hull for the maximum number of days are the highest, is selected for subsequent analysis.

2.3. Skeletonization

The binary plant is skeletonized, i.e., reduced to one pixel-wide lines, using the fast marching distance transform method due to its robustness to noisy boundaries, im-

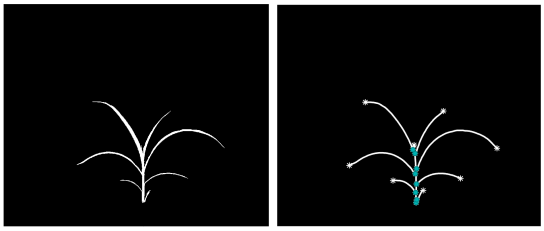

(a) (b)

Figure 3. Illustration of skeletonization: (a) binary image; and (b) skeleton image with junctions and tips marked.

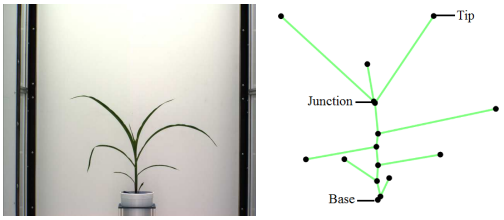

(a) (b)

Figure 4. Illustration of graphical representation of a plant: (a) original plant image; and (b) graphical representation with marked base, tip and junction.

proved skeleton connectivity and low computational complexity [4]. Figure 3(a) shows the binary image of a maize plant and Figure 3(b) shows the corresponding skeleton image.

2.4. Plant body-part labelling

The plant P is represented by a graph, i.e., P={V, E}, where V and E respectively denote the sets of vertices and edges. V={B, J, T}, where B is the bottom-most point of the skeleton which is termed as the base of the plant. It is the special point from which the stem of the plant originates. J denotes the junctions at which the leaves of the plant are connected to the stem and T denotes the tips, i.e., the free endpoints of the leaves. J and T are identified based on analyzing degree of vertices, i.e., if the vertices have degree 3 or more, they are denoted as junctions (J), whereas vertices with degree 1 are denoted as T. E={L, I}, where L denotes the leaves (part of skeleton enclosed between tip and junction) and I denotes the internodes (part of stem enclosed between two junctions). The leaves are identified by starting at the tips and traversing along the skeleton until it meets at a junction. The skeletonization process often results in spurious branches forming degree 3 nodes which are not junctions. Thus, we use a thresholding based skeleton pruning to get rid of spurious branches of length k pixels, where the value of k is chosen as $k \leq 10$ as this value removes most of the spurious branches in this work. Figure 4(a) and (b) respectively show the original plant image and its corresponding graphical representation with base, tip and junctions marked.

2.5. Stem angle measurement

We define stem axis as the straight line formed by linear regression curve fitting of all junctions and the base of a stem. The stem angle (ϕ) is defined as the angle between the stem axis and the vertical axis using

$$\phi = tan^{-1}(m), \tag{1}$$

where m is the slope of the stem axis.

Figure 5 shows the values of stem angle for the plant ID: Plant_006 − 25 of the Panicoid Phenomap-1 dataset for the side view 0° for increasing days. The junctions are shown using red bullets in the figure, while the stem axis is displayed using blue straight line. The stem angle away from vertical axis in the left direction is considered as positive, and the right direction is considered as negative. The values of stem angle are measured in radians.

3. Time series analysis

Plants are dynamically changing organisms with increasing physiological and architectural complexity. Like the plant, its phenotypes also change throughout its life cycle. Therefore, temporal phenotypes may encode significant genetic influences along with the responses to abiotic conditions. In this paper, we present a foundation of several types of time series analyses of component phenotypes, using stem angle as a reference. In particular, our time series analysis (TSA) algorithm includes time series clustering, cluster purity analysis and angular histogram computation. The algorithm for TSA is provided in Algorithm 2.

A time series clustering analysis is performed on the stem angles of the plant. Pearsons correlation coefficient is used as the similarity measure. Silhouette width [9] has been used to determine the optimal number of clusters [2]. Purity is an external validity measure of cluster quality [11], which we have extended here to measure genotype homogeneity of the stem angle time series groups. Purity will have a value ranging from 0 to 1.0. A value of 1.0 implies, all the plants belonging to that particular genotype displays similar temporal pattern of the stem angle. The cluster behavioral patterns are investigated with respect to angular histograms of representative plants. The detailed explanation with graphical illustrations are provided in Section 4.

4. Experimental analysis

4.1. Dataset

Experimental analyses are performed on the Panicoid Phenomap-1 dataset [3]. The dataset can be freely downloaded from http://plantvision.unl.edu/. The images of the

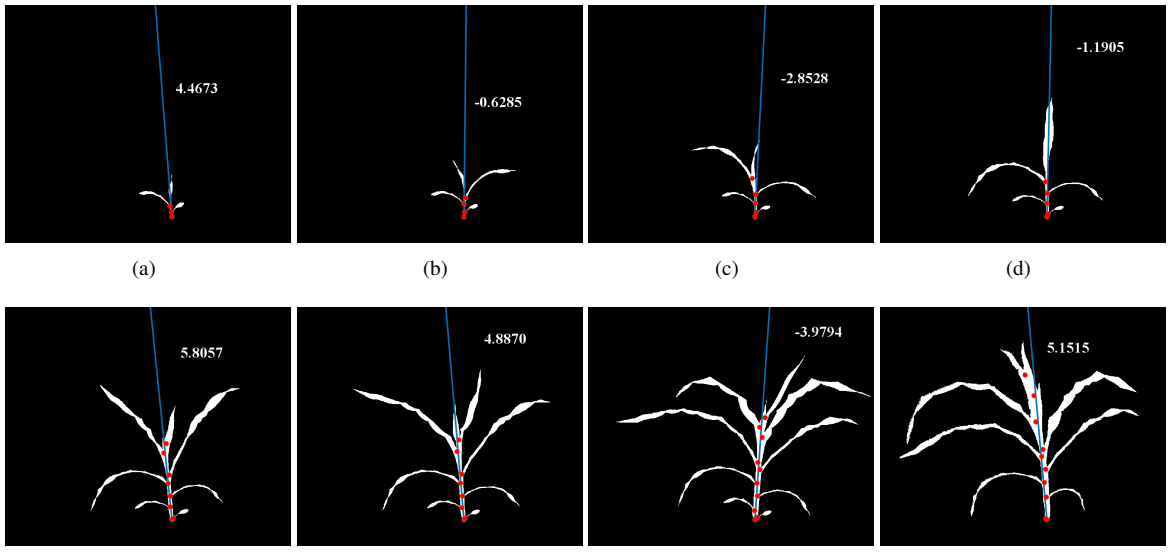

(a) (b) (c) (d)

(e) (f) (g) (h)

Figure 5. Stem angle of a maize plant on different days: (a) Day 7; (b) Day 10; (c) Day 13; (d) Day 16; (e) Day 19; (f) Day 21; (g) Day 25; and (h) Day 27.

Algorithm 2 TSA

Input: A set of plant sequences, i.e., $P = \{P_1, P_2, ..., P_l\}$, where l is the total number of plant sequence. $P_i = \{sa_{i,1}, sa_{i,2}, ..., sa_{i,m}\}$, for i=1,...,l. m represents total number of images in each plant sequence.

Output: Plants distributed into clusters, cluster purity and angular histogram.

Time series cluster analysis

$$\text{C} = \text{Cluster}(P) \tag{2}$$

Where C = {C_1,C_2,...,C_k}, k = optimal number of clusters (3)

Cluster purity analysis

for i=1:k **do**

$$\text{Cp}_\text{i} = \text{ComputeClusterPurity}(\text{C}_\text{i}) \tag{4}$$

end for

Angular histogram analysis

for i=1:n **do**

$$\text{Cah}_\text{i} = \text{ComputeAngularHistogram}(P_\text{i}) \tag{5}$$

end for

dataset are captured by the visible light camera of the Lemnatec Scanalyzer 3D high throughput plant phenotyping facility in the University of Nebraska-Lincoln, USA, once daily for 26 days for two side views, i.e., side view 0° and side view 90°, and a top view starting after two days of germination. Panicoid Phenomap-1 consists of images of 40 genotypes of 176 total number of plants including at least one representative accession from five panicoid grain crops: maize, sorghum, pearl millet, proso millet and foxtail millet. Thus, the dataset contains 26 × 3 = 78 images for 3 views (side view 0°, side view 90° and top view) for a plant, totaling 78 × 176 = 13728 images. Out of 40 genotypes, the dataset contains 32 genotypes of the maize plants. Table 1 shows the genotype names corresponding to genotype IDs used in the dataset. The detailed descriptions of the data capturing process and dataset organization can be found in [3].

4.2. Performance evaluation of SAC

The plants are tiny before Day 7. Thus, the proposed method is evaluated on the images of two side views of the maize plants of Panicoid Phenomap-1 from Day 7 until Day 26. The performance of the proposed method depends on how accurately the junctions are identified. The junctions are often hidden by the leaves, or falsely detected due to leaf crossovers, which lead to failure cases. The accuracy of the SAC method is given by

$$\text{Accuracy} = \frac{t_s}{t_n}, \tag{6}$$

where, t_s denotes the total number of success cases and t_n denotes the total number of images used to evaluate the method. There are 158 total number of maize plants of 32 genotypes in Panicoid Phenomap-1 dataset. Since, we

Table 1. The genotype names corresponding to the genotype IDs used in the Panicoid Phenomap-1 dataset.

G_{ID}	G_{name}	G_{ID}	G_{name}	G_{ID}	G_{name}	G_{ID}	G_{name}	G_{ID}	G_{name}
1	740	9	C103	17	LH82	25	PHG83	33	Yugu1
2	2369	10	CM105	18	Mo17	26	PHJ40	34	PI614815
3	A619	11	LH123HT	19	DKPB80	27	PHH82	35	PI583800
4	A632	12	LH145	20	PH207	28	PHV63	36	Purple Majesty
5	A634	13	LH162	21	DHB47	29	PHW52	37	BTx623
6	B14	14	LH195	22	PHG35	30	PHZ51	38	PI535796
7	B37	15	LH198	23	PHG39	31	W117HT	39	PI463255
8	B73	16	LH74	24	PHG47	32	Wf9	40	PI578074

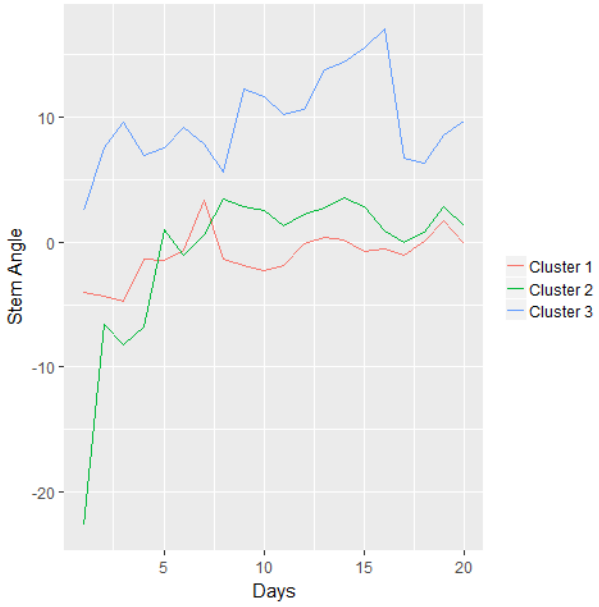

Figure 6. Time series cluster analysis of stem angles.

considered 20 images for each plant (starting from Day 7 to Day 26 both days inclusive, for a single side view), the total number of images used to evaluate the method, i.e., t_n is 158 $\times$ 20 = 3160. The total number of images for which stem angles have been computed successfully, i.e., t_s is 2663. Thus, the accuracy of the SAC method is 84%.

4.3. Time-series cluster analysis

The results of clustering analysis is shown in Figure 6. It is evident from the Figure 6 that the stem angle of the plants in Cluster 1 increased over time, plants in Cluster 2 remains kind of range bound with an upward trend and plants in Cluster 3 shows a downward movement. Cluster 3, exhibited most variation in terms of stem angle.

Table 2 shows the distribution of genotypes in the major clusters. The following observations are made from this table:

- Cluster 1: Majority of the plants of the 7 gentoypes included in this cluster shows an increasing trend of stem angle.
- Cluster 2: Majority of the plants of the 7 gentoypes included in this cluster shows a gradual upward movement, with values of stem angle lower than that of Cluster 1.
- Cluster 3: majority of the plants of the genotypes included in this cluster shows a downward movement of the stem angles over time.
- Unpredictable: Majority of the plants of 6 genotypes in this group shows that there is no conclusive trend of the stem angle movement over time.

4.4. Cluster purity analysis

The time series cluster analysis of stem angle of the plants measured over the vegetative stage life cycle, shows significant variability between the plants. A clustering analysis reveals that there are three fundamental patterns of the time series movement. Next, influence of the genotype on the stem angle time series is investigated. It may be assumed that plants from the same genotype will exhibit similar time series patterns. This assumption in tested with purity analysis of the genotypes. The results of purity analysis with respect to different genotypes are presented in Table 3.

The purity of ith genotype is measured as

$$\frac{\max(g_{i,j})}{\sum g_{i,j}}, \tag{7}$$

where, $g_{i,j}$ represents the number of plants of genotype i present in Cluster j. This is compared against the purity obtained through random assignment of the clusters. The results of analysis is shown in Figure 7 using a box-plot. The figure indicates strong genotypic influence on the time series of the stem angles.

The time series clustering analysis has the potential to provide significant information to the plant scientists. The higher the value of the purity for a particular genotype, more is the degree of homogeneity between the plants. It is observed that, for 25 out of the 31 genotypes, the stem angle

Table 2. Semantic analysis of the Genotypes

Cluster	Cluster Semantics	Genotype
1	Stem angle reducing over time	{2,14,15,20,23,27,29}
2	Stem angle shows a range bound movement	{3,12,16,17,22,25,26}
3	Stem angle shows an uptrend	{1,5,6,7,10,11,13,21,24,28,30}
Unpredictable	No clear majority trend	{4,8,9,18,19,32}

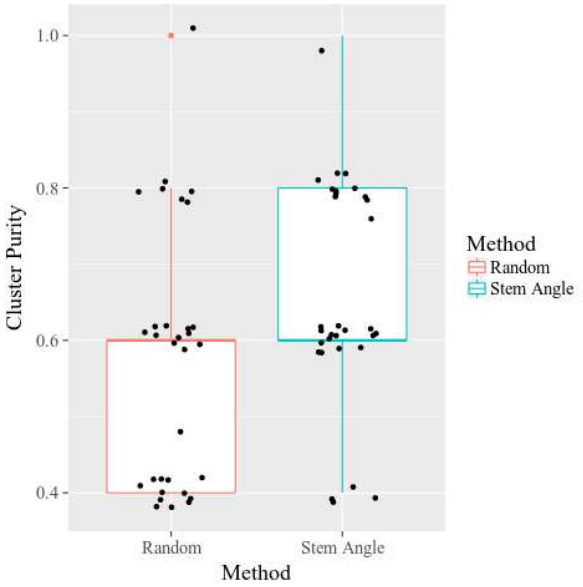

Figure 7. Analysis of genotypic influence on stem angle using boxplot.

Table 3. Genotype-wise purity analysis

Purity	Genotype
1.0	{21,22,26}
0.8	{10,11,13,14,16,24,28}
0.6	{1,2,3,5,6,7,12,15,17,20,23,25,27,29,30}
0.4-0.5	{4,8,9,18,19,32}

time series behavior of the plants in that genotype is homogeneous. For genotyeps 21, 22 and 26, the temporal behavior of the stem angle is completely homogeneous, while for other genotypes, majority of the plants belonging to a particular genotype show similar temporal patterns.

4.5. Angular histogram analysis

Figure 8(a), (b) and (c) respectively show the angular histograms of stem angle distributions of three representative plants from each of three clusters, i.e., plant_185 from Cluster 1, plant_74 from Cluster 2 and plant_102 from Cluster 3. The following observations are made from the figure: (a) Cluster 1 has as almost equal distribution between positive and negative stem angles with positive being more in proportion (see Figure 8(a); in Cluster 2, most of the stem angles are negative with a small percentage being positive (see Figure 8(b)) and (c) Cluster 3 has almost equal distribution between positive and negative stem angles with negative being more in proportion (see Figure 8(c)).

4.6. Run-time complexity analysis

SAC is implemented using Matlab R2017a. The execution time for the stem angle measurement to compute and display stem angle given a sequence of 20 original plant images as the input (starting from Day 7 to Day 26, both inclusive), using an Intel(R)Core(TM) i5 processor with 8 GB RAM working at 2.30-GHz using 64 bit Windows 10 operating system is 19 minutes. This time is reported based on plant ID $Plant\_191 - 28$ for side view $0°$. Thus, the average execution time for a single image is: 57 seconds.

5. Conclusion

The paper introduces a novel 2-phase method called SAC to compute stem angle by analyzing image sequence of a maize plant captured by visible light camera. In phase 1, the view of the plant image at which the line of sight of the camera is perpendicular to the axis of the plant, is selected, and in phase 2, the value of stem angle is measured using the selected view of the plant image. From the perspective of plant science, stem angle is a very significant phenotype, as it contributes in the determination of stem lodging due to high population density, extremes in soil moisture, nutrient deficiency and hybrid susceptibility. SAC uses a graph theoretic approach following skeletonization of the binary plant image to identify the junctions, i.e., the points of contacts of the leaves to the stem. A regression line curve fitting of the junctions is used to form the stem axis, and the stem angle is computed as the angle between the stem axis and the vertical axis in either direction. SAC achieves 84% accuracy on publicly available data set Panicoid Phenomap-1.

The paper also introduces an algorithm for time series analysis (TSA) to investigate the genetic influence on the temporal behavioral pattern of the phenotypes for a significant time interval during vegetative stage life cycle of the maize plants. The effectiveness of this algorithm is investigated using stem angle in this paper, however, it could be extended to any other component phenotype as a foundation for the investigation of phenotype-genotype relationship us-

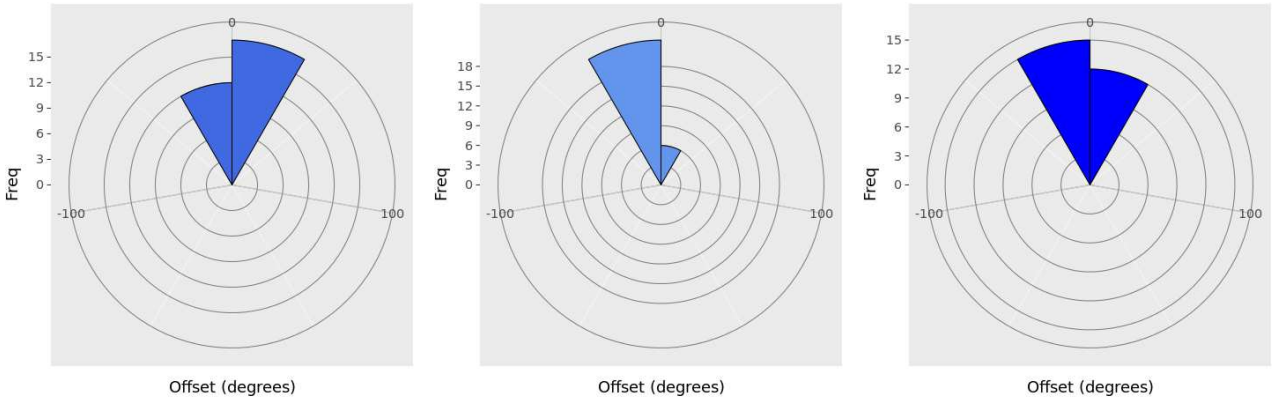

(a) (b) (c)

Figure 8. Angular histograms of stem angles for three representative plants of each cluster: (a) Plant_185 for Cluster 1; (b) Plant_074 for Cluster 2; and (c) Plant_102 for Cluster 3.

ing imaging techniques. TSA involves time-series clustering along with purity analysis and also angular histogram analysis.

In the future work, we will perform similar time-series analysis on a new dataset to study the difference in the response of stem angle to the normal and excess watering conditions of the maize plants regulated by genetic variation. We will also develop algorithms to compute new component phenotypes related to other parts of a plant, e.g., leaf, fruit and flower. The time-series analysis presented in this paper, will be extended to other component phenotypes to investigate their temporal variations regulated by genotypes. SAC algorithm deals with the single view image (at which the line of sight of the camera is perpendicular to the line of axis of the leaves) in the 2D space, and thus unable to account for stem lodging towards and away from the camera. The robustness of the algorithm will be enhanced by employing multi-view image sequence analysis to account for stem lodging in any direction in the range [0° 360°].

Acknowledgments

The authors would like to thank the Agricultural Research Division in the Institute of Agriculture and Natural Resources of the University of Nebraska-Lincoln, USA, for providing the funds for this research.

References

[1] E. E. Aksoy, A. Abramov, F. Wörgötter, H. Scharr, A. Fischbach, and B. Dellen. Modeling leaf growth of rosette plants using infrared stereo image sequences. *Computers and Electronics in Agriculture*, 110:78–90, 2015.

[2] N. Bolshakova and F. Azuaje. Cluster validation techniques for genome expression data. *Signal Processing*, 83(4):825–833, 2003.

[3] S. D. Choudhury, V. Stoerger, A. Samal, J. C. Schnable, Z. Liang, and J.-G. Yu. Automated vegetative stage phenotyping analysis of maize plants using visible light images. In *KDD workshop on Data Science for Food, Security and Water, San Francisco, California, USA*, 2016.

[4] M. S. Hassouna and A. A. Farag. Multi-stencils fast marching methods: a highly accurate solution to the eikonal equation on cartesian domains. *IEEE Transactions on Pattern Analysis and Machine Intelligence*, 29(9):1563–1574, 2007.

[5] M. Jansen, F. Gilmer, B. Biskup, K. A. Nagel, U. Rascher, A. Fischbach, S. Briem, G. Dreissen, S. Tittmann, S. Braun, I. D. Jaeger, M. Metzlaff, U. Schurr, H. Scharr, and A. Walter. Simultaneous phenotyping of leaf growth and chlorophyll fluorescence via growscreen fluoro allows detection of stress tolerance in arabidopsis thaliana and other rosette plants. *Functional Plant Biology*, 36:902–914, 2009.

[6] L. Jianzhuang, L. Wenqing, and T. Yupeng. Automatic thresholding of gray-level pictures using two-dimension otsu method. In *International Conference on Circuits and Systems*, pages 84–89. China, March 1991.

[7] M. Minervini, M. M. Abdelsamea, and S. A. Tsaftaris. Image-based plant phenotyping with incremental learning and active contours. *Ecological Informatics*, 23:35–48, 2014.

[8] B. Nielsen and D. Colville. Stalk lodging in corn: guidelines for preventive management. *AY-Purdue University Cooperative Extension Service (USA)*, 1986.

[9] P. J. Rousseeuw. Silhouettes: A graphical aid to the interpretation and validation of cluster analysis. *Journal of Computational and Applied Mathematics*, 20:53–65, 1987.

[10] H. Scharr, M. Minervini, A. P. French, C. Klukas, D. M. Kramer, X. Liu, I. Luengo, J. Pape, G. Polder, D. Vukadinovic, X. Yin, and S. A. Tsaftaris. Leaf segmentation in plant phenotyping: a collation study. *Machine Vision and Applications*, 27(4):585–606, May 2016.

[11] P.-N. Tan, M. Steinbach, and V. Kumar. *Introduction to Data Mining*. Pearson, 2005.